

## PAST, PRESENT, AND NEW CHALLENGES FOR COMPUTATIONAL HEMODYNAMICS OF CEREBRAL CIRCULATION

Marie OSHIMA<sup>1</sup>, Changyoung YUHN<sup>2</sup>, Masaharu KOBAYASHI<sup>3</sup>

<sup>1</sup> Corresponding Author. Interfaculty Initiative in Information Studies, the University of Tokyo, 4-6-1 Komaba, Meguro-ku, Tokyo, Japan 153-8505 Tel.: +81 3 5452 6205, E-mail: marie@iis.u-tokyo.ac.jp

<sup>2</sup> Institute of Industrial Science, the University of Tokyo (Currently, Toyota Central R&D Labs., INC.). E-mail: yuhn@iis.u-tokyo.ac.jp

<sup>3</sup> Institute of Industrial Science, the University of Tokyo (Currently, Chi Co., LTD). E-mail: mkoba@iis.u-tokyo.ac.jp

### ABSTRACT

A patient-specific simulation has been widely used not only for scientific study to elucidate mechanism between hemodynamics and cardiovascular diseases such as stroke but also for clinical applications to predict post-operative blood flow situation. Since carotid artery stenosis is a major cause of a stroke, patients with severe carotid artery stenosis often undergo revascularization surgery such as carotid artery stenting to prevent a stroke from happening in the future. However, some patients suffer from complications like cerebral hyperfusion syndrome (CHS), which leads to hemorrhage due to a sudden increase in a flow rate in the brain. Therefore, predicting the blood flow in the brain after the surgery is very important to determine the most suitable surgery for an individual patient to avoid complications like CHS after the surgery.

The paper reviews the patient-specific simulation. In order to predict the post-operative flow in the brain after the surgery, it is necessary to consider the entire circulatory system because the surgery affects the blood flow in the brain as well as in the entire circulatory system. Therefore, the authors have been developing a multi-scale blood flow simulation by combining 1D (One-dimensional) and 0D (Zero-dimensional) models.

The patient-specific simulation utilizes geometric and physiological parameters derived from clinical data for the region of interest, i.e. the circle of Willis (CoW) in this paper as well as the literature data for the rest of circulatory system. These data contain uncertainties, which affect the simulation results by propagating through mathematical models and the simulation. Thus, quantifying an impact of uncertainties in medical images on simulated quantities is an essential task to obtain reliable results. In general, uncertainty quantification requires a large number of case studies to investigate the effects of uncertainties in a probabilistic manner. Thus, a surrogate model based on a machine learning

technique was developed and applied to three patients for investigation of CHS risk after the surgery.

**Keywords:** patient-specific simulation, multi-simulation, 1D-0D models, quantification of uncertainties, machine learning, cerebral circulation

### 1. INTRODUCTION

Stroke is the second cause of death in the world [1]. It is not only fatal because of high mortality rate but also low quality of life in case of severe complications such as parallelization or impaired consciousness. There are two types of strokes: ischemic and hemorrhage strokes. The ischemic strokes are mainly caused by severe arterial stenosis, which is resulted from progression of atherosclerosis. The arterial stenosis is a serious cardiovascular disease-causing large pressure drop and an abrupt decrease in a flow rate. If stenosis becomes highly severe, a surgery such as carotid artery stenting (CAS) or carotid endarterectomy (CAE) is performed to prevent those fatal situations[2,3]. However, the surgery sometimes causes the postoperative syndrome such as intracranial hemorrhage caused by cerebral hyperfusion (CHS) [4]. Thus, it is important to examine the effects of surgery on a patient and to understand changes in the distributions of blood flow and pressure after the surgery.

The patient-specific modeling and numerical simulations have been widely applied to investigate the hemodynamics for an individual patient [5, 6]. In this method, the simulation is performed in the three-dimension for the patient's vascular geometry, which is constructed from the medical images such as computed tomography (CT) or magnetic resonance imaging (MRI). It can provide the detailed hemodynamic information but limited only to the region of interest due to resolution of the medical images. The surgery influences hemodynamics not only in a localized region around the stenotic region,

in which medical images are available but also throughout the peripheral areas to the entire circulatory system. The objective of the paper is to develop a simulation system to examine the hemodynamics locally as well as globally in the circulatory system. Thus, a multi-scale approach has been developed to consider the effects of peripheral vascular network as well as the entire circulatory system using combined reduce models of one-dimension (1D) and zero-dimension (0D) [7-9]. The 1D-0D simulation is an appropriate method to capture primary hemodynamics information such as flow rate or pressure with less computing time and better portability comparing to three-dimensional (3D) simulation.

The Patient-specific blood flow simulation is performed by applying vascular geometry and velocity information from medical images of an individual patient to obtain hemodynamic factors such as blood flow velocity, pressure, and wall shear stresses, which are important indicators for cardiovascular diseases. The pipeline of the patient-specific simulation system consists of three steps: 1) vascular geometric modeling, 2) multi-scale blood simulation using multi-modal data of medical images, and 3) visualization of simulation results as illustrated in Figure1[8].

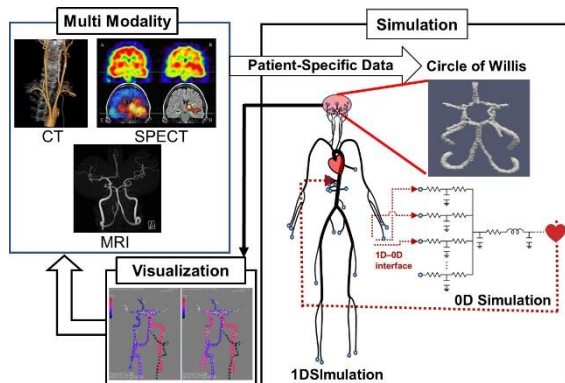


**Figure1. Schematic illustration of patient-specific simulation**

In the first step for vascular geometric modeling, the 3D vascular geometry is constructed from either CT or MRI. The information on the radius and the length of artery can be obtained as well as the vascular parameter such curvature and torsion from the 3D vascular geometry data and it is applied to a part of 1D domain in order to perform the patient-specific 1D-0D simulation. In the second step for multi-scale blood simulation using multi-modal data of medical images, the simulation can be conducted in either 1D-0D or 3D-1D-0D depending on how detail the hemodynamic information is required. Since the 1D-0D simulation is carried out with consideration of the entire circulatory system incorporating the patient-specific geometry constructed from the medical images, it is quite effective to examine the influences of surgery for each

patient. In the last step for visualization, it is important to present the simulation results in an effective way for better understanding of hemodynamics or for an appropriate diagnosis to provide a suitable surgical planning. However, the current visualization tools are generally available for the 3D simulations but not for the 1D-0D simulation. Therefore, the authors have been developing a visualization system for the 1D domain where the patient-specific geometry is applied.

The present simulation system was applied to investigate the blood flow in the Circle of Willis (CoW), which is a vital region of cerebrovascular circulation. The paper presents each process in the pipeline of patient-specific simulation using 1D-0D simulation with multimodal data of medical images. The results were compared between pre- and post-operative flows to examine the effects of revascularization surgery on cerebral circulation[8].

Since the patient-specific simulation is generally carried out using patient data, the uncertainties in the data propagate throughout mathematical models as well as the simulation and affect the simulations results. Therefore, uncertainty quantification (UQ) is an important issue, particularly for clinical applications. In the paper, the UQ is performed using a machine-learning surrogate model based on the 1D-0D simulation of the cerebral circulation with consideration of the entire circulatory system to estimate the flow rates in the Circle of Willis (CoW) for prediction of CHS risk. The CHS occurs when the post-operative flow rate becomes larger than 100% of the pre-operative one, in which the post-operative flow rate becomes twice the pre-operative one [4]. Thus, in this study, a difference in flow ( $\Delta Q$ ) between before and after the surgery was predicted. Since the UQ requires a large size of simulations, a surrogate model has been developed using deep neural network (DNN) with the datasets obtained from the 1D-0D simulation. The accuracy of surrogate model was investigated by varying hyperparameters and the number of training data. The present surrogate models were applied to three patients including one patient with high risk of CHS. The results showed that the surrogate model predicted probabilistic distribution of  $\Delta Q$  in each artery of CoW with drastic reduction in computer time from twenty- minutes of 1D-0D simulation to milliseconds.

## 2. VASUCULAR GEOMETRIC MODELING

The vascular geometric modelling plays an important role in the patient-specific simulations. The authors have been developing a vascular geometric modelling system, V-Modeler [10,11]. The vascular geometry is extracted from the medical images of DICOM data format such as CT or MRA. V-Modeler conducts the modeling procedure according to the

five processes: (I) segmentation of arterial lumen, (II) extraction of luminal centerlines, (III) reconstruction of surfaces, (IV) calculation of geometrical parameters, and (V) registration and tracking of centerlines and surfaces. If there are series of medical images in time, the temporal changes in geometry can be captured in a parametric manner.

The arterial lumen is segmented from each slice of medical images in process I. After the centerlines are extracted from the segmented regions in the process II, they are converted into spline functions. In the process III, the 3D surfaces of the lumen are constructed. The process IV provides the geometric parameters of the lumen and its centerlines such as the length of centerline, radius of the lumen on each cross section perpendicular to the centerlines. The 3D geometric parameters of curvatures and the torsions are also calculated along the centerlines. In the process V, registration is performed so as to determine a geometrical transformation by aligning corresponding points between two sets of the same modality of medical images.

The development environment of V-Modeler is based on Visual Studio 2010 Professional (C++ programming language) on Windows 7 Professional 64bit. The image processing libraries are MIST (Media Integration Standard Toolkit, Nagoya University, Japan) and OpenCV 2.2, visualization library is OpenGL. The GUI of V-Modeler is designed to perform each process interactively and user-friendly, and to visualize the results of CoW as described in Figure 2. The vascular geometry of Figure 2 was extracted from MRA of the patient, who was a 70 years old male with 73%(NASCET) stenosis on the left ICA( Internal Carotid Artery) and had CAS surgery for revascularization treatment.

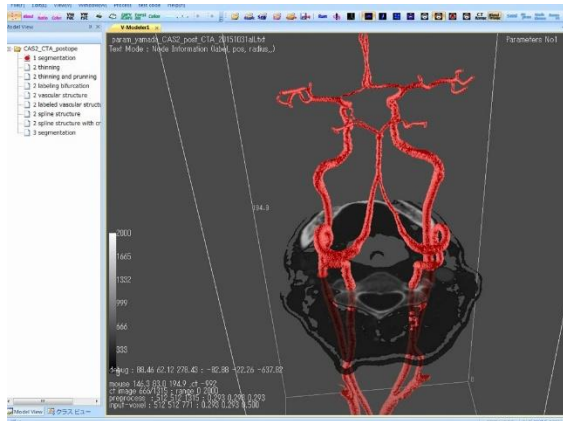


**Figure2. The circle of Willis constructed from MRA using V-modeler**

In order to derive a smooth centerline against noises intrinsic to the medical images for calculation for curvature and torsion, the authors developed a new penalized SFM, “geo-SFM”. The present method enables us to optimize geometrical parameters such as curvature and torsion along arterial centerlines extracted from medical images using a penalty term

with a higher-order degree of spline as well as Akaike indices to determine the unknown coefficients associated with penalty terms.

For a B-spline curve and its derivatives, let  $\mathbf{P}(t) = (x, y, z)$  be a position vector along a curve as a function of a parameter  $t$  as follows:

$$\mathbf{P}(t) = \sum_{i=1}^n B_{i,k}(t) \mathbf{x}_i, \quad (1)$$

where  $B_{i,k}(t)$  is the  $i$ -th normalized B-spline function of order  $k$  (degree  $k-1$ ), and  $\mathbf{x}_i = (x_i, y_i, z_i)$  is the position vector of the  $n$  control polygon vertices.  $B_{i,k}(t)$  is defined by the Cox-de Boor recursion formulas,

$$B_{i,1}(t) = \begin{cases} 1 & t_i \leq t < t_{i+1} \\ 0 & \text{otherwise} \end{cases}$$

$$B_{i,k}(t) = \frac{(t-t_i)B_{i,k-1}(t)}{k-1} + \frac{(t_{i+k}-t)B_{i+1,k-1}(t)}{k-1}. \quad (2)$$

The  $N$ -th derivative of the B-spline curve  $\mathbf{P}^{(N)}(t)$  with  $t$  is obtained from the  $N$ -th derivative of the B-spline function,  $B_{i,k}^{(N)}(t)$ .

$$\mathbf{P}^{(N)}(t) = \sum_{i=1}^n B_{i,k}^{(N)}(t) \mathbf{x}_i \quad (3)$$

The geometric parameters on the spline curve, such as curvature  $\kappa$  and torsion  $\tau$ , are given respectively by

$$\kappa = \frac{1}{s^2} \sqrt{(x'')^2 + (y'')^2 + (z'')^2}$$

$$\tau = \frac{1}{\kappa^2 s^6} \begin{vmatrix} x' & y' & z' \\ x'' & y'' & z'' \\ x''' & y''' & z''' \end{vmatrix}, \quad (4)$$

where  $x', x''$ , and  $x'''$  are the 1<sup>st</sup>, 2<sup>nd</sup>, and 3<sup>rd</sup> derivative of  $x$  in terms of  $t$ , and  $y', y'', y''', z', z'',$  and  $z'''$  are as well. The variable  $s'$  is defined as,

$$s' = \sqrt{(x')^2 + (y')^2 + (z')^2}. \quad (5)$$

The geo-SFM uses the 5<sup>th</sup> degree spline basis function and penalty terms of both the 3<sup>rd</sup> and 4<sup>th</sup> derivatives to optimize curvature and torsion along the fitted curve. The degree of spline basis function requires the 5<sup>th</sup> degree spline basis function at minimum in order to assure continuity and smooth connectivity of piecewise polynomials with respect to the 3<sup>rd</sup> derivative along the B-spline curve. The penalty terms require the 3<sup>rd</sup> and 4<sup>th</sup> derivatives in order to control the 2<sup>nd</sup> and 3<sup>rd</sup> derivatives of the fitted curve used to calculate the curvature and torsion in (4).

The objective function  $S_{geo}$  of geo-SFM is defined by

$$S_{geo} = \sum_{j=1}^m \{y_j - P(t_j)\}^2 + \lambda_3 \int_{t_{min}}^{t_{max}} \left\{ \frac{d^3 P(t)}{dt^3} \right\}^2 dt + \lambda_4 \int_{t_{min}}^{t_{max}} \left\{ \frac{d^4 P(t)}{dt^4} \right\}^2 dt, \quad (6)$$

where  $\mathbf{P}(t)$  is the fitted curve,  $\mathbf{y}_j$  are  $m$  data points,  $\lambda_3$  and  $\lambda_4$  are the coefficients of the penalty terms determined to minimize the objective function  $S_{geo}$ , and  $t_{min}$  and  $t_{max}$  are integral intervals of the parameter  $t$  of the fitted curve.

The AIC is used to identify optimal penalty terms as a measure of the relative quality of statistical models for a given set of data. Let  $L$  be the Gaussian log-likelihood; AIC is then given by

$$AIC = \sum_{j=1}^m \frac{1}{\sigma^2} (y_j - \sum_{i=1}^n \mathbf{B}_{i,k}(t_j) x_i)^2 + 2m \ln \sigma + 3m \ln 2\pi + 3 \cdot 2 \cdot \text{trace}(\mathbf{H}), \quad (7)$$

where  $\mathbf{H}$  is defined as

$$\mathbf{H} = \mathbf{B}(\mathbf{B}^T \mathbf{B} + \lambda_3 \mathbf{B}_3^T \mathbf{B}_3 + \lambda_4 \mathbf{B}_4^T \mathbf{B}_4)^{-1} \mathbf{B}^T \quad (8)$$

and  $\text{trace}(\mathbf{H})$  in (7) represents the effective dimension.

### 3. NUMERICAL METHOD OF MULTI-SCALE BLOOD SIMULATION

The 1D-0D simulation consists of the closed loop to represent the entire circulatory system in a way that the outflow boundaries of the 1D domain are connected to the inflow boundaries of the 0D domain while the outflow boundaries of the 0D domain are connected to the inflow boundaries of the 1D domain. The 1D simulation is conducted for the blood flow in large arteries while the 0D is for small arteries, arterioles, capillaries, veins, and heart. In the 1D-0D simulation, the statistical data are used for the geometry such as the radius and the length and for the physiological properties such as resistance, compliance, and inductance. The patient-specific geometry is also applied to a part of 1D domain, in this paper, CoW in order to obtain the hemodynamic information for individual patients.

The 1D simulation is applied to a total of 83 arteries which consists of 55 arteries based on Liang model[7] and newly added 27 arteries of cerebrovascular and neck circulations[8]. The governing equations of the 1D simulation can be obtained by integrating the continuity and Navier-Stokes equations over an artery cross-section and are given by [12]:

$$\frac{\partial A}{\partial t} + \frac{\partial Q}{\partial z} = 0 \quad (9)$$

$$\frac{\partial Q}{\partial t} + \frac{\partial}{\partial z} \left( \frac{Q^2}{A} \right) + \frac{A}{\rho} \frac{\partial P}{\partial z} + 8\pi \frac{\mu Q}{\rho A} = 0 \quad (10)$$

where  $A$ ,  $Q$  and  $P$  are the cross-sectional area, the flow rate and the pressure, respectively. In addition, the following pressure-area relationship is used:

$$P - P_0 = \frac{Eh_0}{r_0(1-\sigma^2)} \left( \sqrt{\frac{A}{A_0}} - 1 \right) \quad (11)$$

where  $E$ ,  $h$ ,  $r$ , and  $\sigma$  represent the Young's modulus, the wall thickness and arterial radius, and the Poisson ratio. The subscript 0 means a value at the reference state. Since the artery is an incompressible material, the Poisson ratio in the paper is taken to be 0.5. The Lax-Wendorff method is used to solve equations (1)-(3).

In this study, the patient-specific geometry was applied to the part of CoW. The 1D simulation used the configuration of vascular network in the CoW and the geometric information of the arterial radius and length, in which could be provided easily by the 3D geometric information of V-Modeler.

The 0D simulation is applied to the peripheral vascular network, which consists of arteries smaller than one used for the 1D simulations, capillaries, venous system, and heart. The 0-D simulation is given by lumped parameter models as follows[7,8]:

$$C \frac{dP_i}{dt} + Q_{i+1} - Q_i = 0 \quad (12)$$

$$L \frac{dQ_{i+1}}{dt} = -(P_{i+1} - P_i) - RQ_{i+1} \quad (13)$$

where  $C$ ,  $L$ , and  $R$  represent the compliance, the inductance, and the resistance of the blood vessel. The 4<sup>th</sup> order Runge-Kutta method is used to solve equations (4) and (5).

The 1D model can not capture a pressure drop ( $\Delta P$ ) in a stenosis region caused by separation due to an abrupt change in a cross-sectional area because separation is a three-dimensional phenomenon. Therefore, the following 0D stenosis model by Young and Tsai is applied to the stenosis region [13,14]:

$$\Delta P = R_v Q + K_t \frac{8\rho}{\pi^2 D_n^4} \left\{ \frac{1}{(1-SR)^2} - 1 \right\}^2 Q|Q| + K_u \frac{4\rho L_s}{\pi D_n^2} \dot{Q}, \quad (14)$$

where  $R_v$ ,  $D_n$ ,  $SR$ ,  $L_s$ , and  $\dot{Q}$  are the viscous resistance of the stenosis, the maximum diameter distal to the stenosis, a stenosis ratio defined as the percentage reduction in diameter  $(1 - D_s/D_n)$  with the minimum stenosis diameter  $D_s$ , the stenosis length, and the time derivative of  $Q$ , respectively. The first, second, and third terms in Eq. (14) describe pressure drop by viscous friction, flow separation, and pulsatility, respectively. In this paper,  $R_v$  was given

by Bessems [15] with consideration of the diameter change along the axial direction as follows:

$$R_v = \int_0^{L_s} \frac{128\mu}{\pi D^4(x)} dx, \quad (15)$$

where a parabolic velocity profile (i.e., Poiseuille flow) was assumed throughout the stenosis. The coefficients  $K_t$  and  $K_u$  depend on the stenosis geometry. They were assumed to be 1.52 and 1.2, respectively according to the literature [14,16] while  $K_u$  was fixed as 1.2 due to its negligible influence on  $\Delta P$ . However, in the UQ study,  $K_t$  was regarded as an uncertain parameter ranging between 1.0 and 2.699 [17].

When the patient-specific geometry is applied to the 1D-0D simulation, it is also necessary to adjust the differences in the physiological parameters such as the peripheral resistances from the literature data to the patient-specific ones. In this study, the SPECT data were used as the reference data to adjust the peripheral resistances in the 0D domain downstream from the region where the patient-specific geometry region were applied since they represented a map of the peripheral flow rates in the brain. The PC-MRA data were also used together with the SPECT data in order to predict the flow rate more accurately[8]. In the present method, the peripheral resistance of each efferent artery of the CoW,  $R$  was adjusted in every cardiac cycle to match with the corresponding reference flow rate by the SPECT data  $Q_s$  as follows[8]:

$$R_i^{n+1} = R_i^n \cdot \left(1 - \alpha \cdot \frac{Q_{s,i} - Q_i^n}{Q_{s,i}}\right) \quad (16)$$

where the subscript  $i$  and the superscript  $n$  denote the efferent arterial segment number and the number of the cardiac cycle, respectively. The parameter  $\alpha$  is a relaxation coefficient.

#### 4. VISUALIZATION OF 1D SIMULATION

The commercial software for visualization of results is generally available for the 3D simulation but not for the 1D-0D simulation. In the present simulation, the patient-specific 3D geometry was applied to the CoW region as a part of the 1D simulation. Thus, the paper has developed a visualization system for the 1D simulation where the patient-specific data are used.

The visualization part is incorporated into V-Modeler as described in Figure 3 since the 1D simulation uses the information of the radius and length extracted from the medical image data by V-Modeler [9]. V-Modeler has also the information about the centreline of vascular lumen, which is expressed by a spline-function. First of all, the grid point used for the 1D simulation is allocated in the three-dimensional coordinates using the information of the centreline in the 3D. Since the radius can be

obtained from the area resulted from 1D simulation, the pressure and the flow rate were remapped onto the 3D geometry.

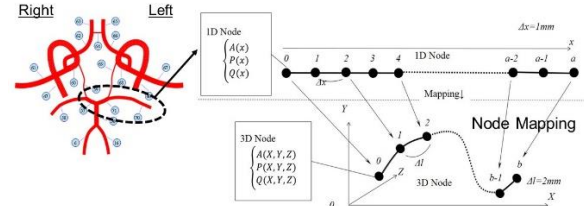
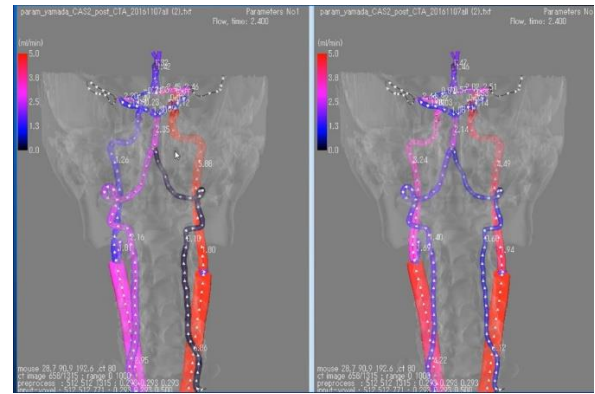


**Figure 3. Schematic illustration of mapping 1D simulation results onto 3D vascular geometry**

Visualization can be carried out not only for the changes in the flow rates, the pressures, and the cross-sectional areas but also for the wall shear stresses, which are post calculated from the results of 1D simulation. The results can be also presented as movie to see dynamic changes of flow. Figure 4 shows the simulation results of pre-operative (Figure 4.A) and post-operative (Figure 4.B) flow rates for the same patient, whose vascular geometry is described in Figure 2.



**A) Pre-operative case B) Post-operative case**  
**Figure 4. Visualisation of flow rates in CoW from the posterior view**

Since there was stenosis on the left ICA, the flow rate on the left side was lower than that on the right side while the flow rate on both sides became the same after the surgery. In general, the flow rates for a healthy person are about equal on both sides so that revascularization surgery was successful.

#### 5. UNCERTAINTY QUANTIFICATION

Even though patient-specific simulations are verified and validated, there is an intrinsic limit to accuracy due to uncertainties in clinical data. For example, a size of each arterial diameter or length in the CoW can be different depending on a person who perform segmentation. These uncertainties come not only from segmentation but also from various sources such as spatial and temporal resolution of medical images, measurement errors, and so on. Therefore, it is necessary to evaluate the simulation results not in a

deterministic but in a stochastic manner by considering uncertainties in clinical data and their non-linear influences through the simulation on results.

However, if such uncertainties are included in the simulation, the computational cost would increase dramatically due to a large number of simulations by varying simulation conditions with many combinations of uncertainties. In order to perform UQ within a reasonable computational, reduction of computational cost is essential. There are two approaches: reduction in the number of simulations or in the cost of an individual simulation. The first one puts an emphasis on the efficiency of the stochastic space using techniques such as stochastic collocation methods [18] or multi-resolution stochastic expansion [19,20] to achieve a faster convergence of statistics. The second one employs reduced-order (1D–0D) models [21,22]. However, UQ still faces a challenge even with reduced order models since individual simulations usually involve iterative calculations to assimilate the data or to obtain converged solutions, which still requires a large amount of time and computational resources.

Due to recent advancement in machine-learning technique, one effective way is to construct a data-driven surrogate model by fitting a regression model to the simulation data. The surrogate model can predict the results based on simple input-output relationships from verified and validated cardiovascular models, which leads to significant acceleration of predictions with sufficient accuracy. Recently, a data-driven machine learning method has been developed using deep neural networks (DNNs) [23–25]. DNNs is effective to map high-dimensional data with complex and highly non-linear relationships. Even though incooperating machine learning techniques to cardiovascular simulations has been an active area of research in the last few years [25–27], most of them have been developed to predict fractional flow reserve in coronary arteries. In this paper, the surrogate model was developed to conduct UQ efficiently even on a PC computer for cerebral circulation, which has complex blood flow patterns because of collateral pathways forming a ring-like structure of CoW.

### 5.1. Surrogate Model based on Machine Learning

The DNN was employed for the surrogate model based on machine learning as a regression model and was fitted to the training data to obtain an input-output relationship from the 1D–0D simulation. After constructing the surrogate model, UQ was conducted following the pipeline described in Figure 5 [28].

In order to develop the surrogate model, acquisition of training data is an important task by defining inputs and outputs. In this study, input data were a total of 60 parameters as follows:

- Diameters of 22 carotid and cerebral arteries in the 1D model (22 parameters).

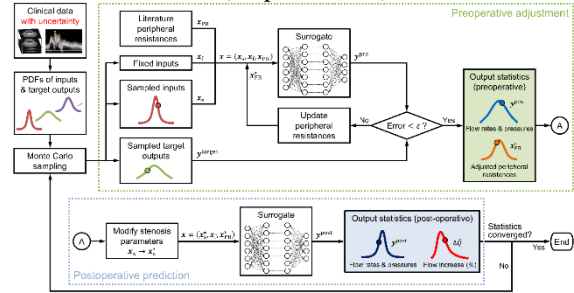


Figure 5. Schematic pipeline of uncertainty quantification [28]

- Lengths of 22 carotid and cerebral arteries in the 1D model (22 parameters).
- $R_v$ ,  $D_n$ ,  $K_t$ , and  $SR$  in Eqs. (14) and (15) for each of the left and right ICA stenoses (8 parameters).
- PRs at the six outlets of the CoW (7 parameters).
- Scaling factor for the total PR (1 parameter).
- Age (1 parameter).

A total of 60 parameters characterized the patient’s anatomical and physiological conditions and also became as inputs to the surrogate model for investigation of UQ in the cerebral circulation. In this paper, variation of stenosis length,  $L_s$ , was ignored because the third term of Eq. (14) was negligible compared to the other terms. However, the effect of  $L_s$  on the viscous resistance of the stenosis was included in  $R_v$ , as seen in Eq. (15).

After the simulation results such as  $A$ ,  $Q$ , and  $P$  were obtained by the present 1D–0D, the following output data were selected for the surrogate model:

- Cycle-averaged flow rates,  $\bar{Q}$ , in the middle of the carotid and cerebral arteries (22 quantities).
- Cycle-averaged pressures,  $\bar{P}$ , in the middle of the carotid and cerebral arteries (22 quantities).
- Mean arterial pressure, i.e., the cycle-averaged pressure in the middle of the left subclavian artery (1 quantity).

A total of 45 output parameters above were the primary clinically relevant quantities of cerebral circulation in this study. Therefore, the surrogate model defined a mapping from the inputs  $\mathbf{x} \in \mathbb{R}^{60}$  to the outputs  $\mathbf{y} \in \mathbb{R}^{45}$ .

After the 1D–0D simulation was performed to create a total of 200,000 sets of input-output varying 60 input parameters, the data set was divided into three groups: 1) training, 2) validation, and test data in a ratio of 6:2:2. The surrogate model was developed using the DNN with 120,000 training data and validated with 40,000 test data. The hyperparameters of DNN such as  $N_{layer}$ ,  $N_{mode}$ ,  $B$ , and  $l_t$  were set to be 7,200, 3,00, and  $10^{-2.5}$ , respectively.

## 5.2. Patient Characteristics

A total of three patients were selected for this study. The characteristic of each patient is summarized in Table 1 and the vascular geometry of each patient is also described in Figure 6.

**Table 1 Characteristics of patients[28]**

	Patient 1	Patient 2	Patient 3	
Age/Sex	82/M	63/M	72/M	
Mean arterial pressure	109.0 mmHg	112.0 mmHg	118.3 mmHg	
Stenosis	Location	Rt. ICA	Lt. ICA	Rt. ICA
	SR	59%	83%	91%
	$R_v$	0.5 mmHg s mL <sup>-1</sup>	11.3 mmHg s mL <sup>-1</sup>	66.6 mmHg s mL <sup>-1</sup>
	Treatment	Endarterectomy	Staged stenting	Endarterectomy
Geometry	CT	CT	CT	
Flow data	Inflow rate	PC-MRI	Doppler ultrasound	PC-MRI
	Outflow rate	SPECT	SPECT	SPECT
Circle of Willis structure	Complete	One artery may be absent	Complete	

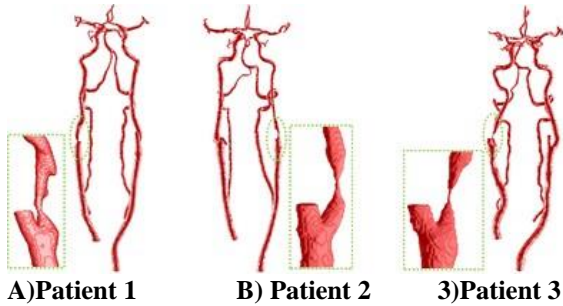


**Figure 6. Vascular geometry[28]**

For all patients, CT data were used to construct vascular geometry while PC-MRI or ultrasound data were used for inflows as well as SPECT data for outflows. The mean arterial pressure in the upper arm were measured before the surgery. The stenosis ratios (SR) for Patients 1–3 were measured as 59%, 83%, and 91%, respectively, which result in the respective values of  $R_v$  as 0.5 mmHg s mL<sup>-1</sup>, 11.3 mmHg s mL<sup>-1</sup>, and 66.6 mmHg s mL<sup>-1</sup>, respectively. Patient 1 and Patient 3 had a complete CoW while Patient 2 was difficult to confirm an anterior communicating artery (ACoA) from CT data. In addition, Patient 2 was identified by the surgeon as high risk for CHS, based on the collected data. In fact, Patient 2 underwent staged surgery, where the stenosis was pre-dilated with a balloon, followed by complete dilation with a stent after two weeks.

## 5.3. Uncertainty Quantification for risk prediction of CHS

The risk of CHS is identified as a drastic increase (>100%) in cerebral blood flow (CBF) immediately after an ICA stenosis surgery [4]. Therefore, if a difference  $\Delta Q$  in flow rates between

per-operative and post-operative flows becomes more than 100%, a patient can be assumed to have high risk of cerebral hyperfusion status. Therefore, the following quantity is evaluated as an indicator:

$$\Delta \bar{Q}_i = \frac{\bar{Q}_i^{\text{post}} - \bar{Q}_i^{\text{pre}}}{\bar{Q}_i^{\text{pre}}} \times 100\%, i = 1, 2, \dots, 6 \quad (17)$$

where  $\bar{Q}_i^{\text{pre}}$  and  $\bar{Q}_i^{\text{post}}$  denote the cycle-averaged flow rates at the six outlets of the CoW before and after dilating the stenosis, respectively.

Since the arterial diameter or length was obtained from CT, its uncertainty associated with CT was defined with  $\pm 2$  pixels ( $\pm 0.702$ – $0.936$  mm, depending on image resolution) with respect to the arterial diameter obtained from segmentation. The uncertainty in the stenosis parameters was considered to be a 2-pixel except Patient 2, whose the anterior communicating artery (ACoA) was too difficult to be segmented from CT images. Hence, we assumed its diameter had an uncertainty of 0.1–2.6 mm, which included the possibility that the artery was absent.

The uncertainties in the measured flow rates were determined depending on the modality. The uncertainty in each modality was defined as  $\pm 16\%$  for PCR-MRI,  $\pm 35\%$  for ultrasound, and  $\pm 16\%$  for SPECT. These ranges were determined based on the literature [8].

The Monte-Carlo method was used to evaluate propagation of uncertainties and their influences on the predicted  $\Delta \bar{Q}_i$ . The surrogate model reduced significantly the time and computational costs required for UQ to several milliseconds on a single core of the CPU (Intel Core i9-9900K). In this study, a GPU machine (NVIDIA GeForce RTX2080 Ti) was used to perform 10,000 parallel predictions on a GPU, which resulted in more significant reduction of computer time.

Figure 7 summarizes  $\Delta Q$ , an increase in flow rate from pre- to post-operation at the middle cerebral artery on the stenosis side.

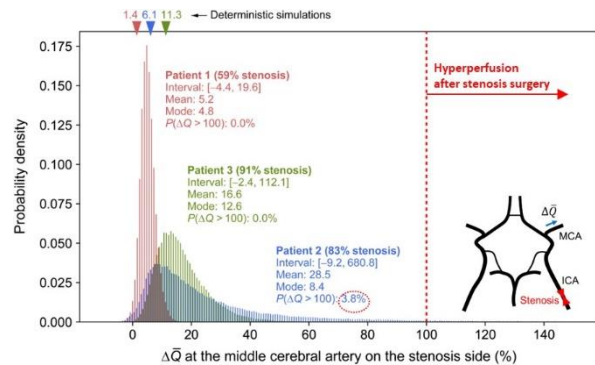


**Figure 7. Comparison of probability density of an increase in flow rate from pre-operative to the post-operation ( $\Delta Q$ ) for Patient 1-3[28]**

As shown in Figure 7, large variations were found in the predicted  $\Delta \bar{Q}$  by considering uncertainties.

The distribution of  $\Delta\bar{Q}$  showed more extensive spread, especially to high values, in Patients 2 and 3 with more severe stenosis (83% and 91% stenosis, respectively) than in Patient 1 (59% stenosis). Since Patient 2 had a large uncertainty in the diameter of the ACoA, a pronounced variability of  $\Delta\bar{Q}$  (up to 681%) was observed, which implied that  $\Delta\bar{Q}$  was significantly affected by this artery. In addition, Patient 2 might have a 3.8% chance of  $\Delta\bar{Q}$  exceeding 100% while the corresponding estimates for Patients 1 and 3 were 0% and 0.001% (only one sample), respectively.

## 6. SUMMARY

The paper presented a multi-scale 1D-0D simulation method with multimodal medical images. In order to conduct uncertainty quantification, a data-driven surrogate model was developed using a machine learning technique. The risk of CHS was predicted by training a DNN with 1D-0D simulation data. The surrogate model reduced the time required for a prediction to a few milliseconds. The present surrogate model was applied to the UQ problem by evaluating the impact of uncertainties in the arterial diameters, stenosis parameters, and measured flow rates on the predicted increase in CBF ( $\Delta\bar{Q}$ ) following carotid artery stenosis surgery. Due to the excellent parallelization performance, the surrogate model enabled UQ with 100,000 predictions to be performed in less than a minute. A high  $\Delta\bar{Q}$  of more than 100% was observed when the stenosis ratio was high and the ACoA had a small diameter, which suggested that severe stenosis with insufficient collateral circulation may be a risk factor for CHS.

Even though the paper showed only CHS case, the surrogate model can be applicable more broadly to prediction of cerebral circulation. The proposed surrogate modeling approach will facilitate the execution of not only UQ but also other computationally expensive tasks such as sensitivity analysis and extensive case studies to advance applying simulation to clinical study.

## ACKNOWLEDGEMENTS

This work was supported by the Japan Society for the Promotion of Science through Grants-in-Aid for Scientific Research (Grant Nos. 16H04264 and 18J21374). The authors would like to acknowledge Dr. Shigeki at Shiga University of Medical Science and Motoharu Hayakawa at Fujita Health University for their support to provide medical images.

## REFERENCES

[1] WHO (World Health Organization) , ‘‘The top cause of death’’, <https://www.who.int/news-room/fact-sheets/detail/the-top-10-causes-of-death>.

[2] North American Symptomatic Carotid Endarterectomy Trial Collaborators, Barnett HJM, Taylor DW, et al. , 1991, ‘‘Beneficial Effect of Carotid Endarterectomy in Symptomatic Patients with High-grade carotid stenosis’’, . *N Engl J Med*. Vol. 325, pp.445-453.

[3] Brott, T. G., Hobson, R.W. 2nd, Howard, G., et al., 2010, ‘‘ Stenting versus Endarterectomy for Treatment of Carotid-Artery Stenosis’’. *N Engl J Med*. Vol.363, pp.11-23.

[4] van Mook, W. N., Rennenberg, R. J., Schurink, G. W., et al. 2005, ‘‘Cerebral Hyperfusion Syndrome’’. *Lancet Neurol.*, Vol.4, pp.877-888.

[5] Oshima, M., Torii, R., Tokuda, S., Yamada, S., Koizumi, A.,2012, ‘‘Patient-Specific Modeling and Multi-Scale Blood Simulation for Computational Hemodynamic Study on the Human Cerebrovascular System’’, *Current Pharmaceutical Biotechnology*, Vol.13, pp. 2153-2165.

[6] Grinberg, L., Cheever, E., Anor, T., Madsen, J. R., Karniadakis, G. E., 2011, ‘‘ Modeling Blood Flow Circulation in Intracranial Arterial Networks: a Comparative 3D/1D Simulation Study’’, *Ann Biomed Eng*. Vol. 39, pp.297-309.

[7] Liang, F., Oshima, M., Huang, H., Liu, H., Takagi, S., 2015, ‘‘Numerical Study of Cerebroarterial Hemodynamic Changes Following Carotid Artery Operation: A Comparison Between Multiscale Modeling and Stand-Alone Three-Dimensional Modeling’’, *Journal of Biomechanical Engineering*, Vol.137, DOI: 10.1115/1.403145.

[8] Zhang, H., Fujiwara, N., Kobayashi, M., Yamada, S., Liang, F., Takagi, S., Oshima, M., 2016, ‘‘Development of a Numerical Method for Patient-Specific Cerebral Circulation using 1D-0D Simulation of the Entire Cardiovascular System with SPECT Data’’, *Annals of biomedical engineering*, Vol.44, pp. 2351-2363.

[9] Yuhn, C., Hoshina, K., Miyahara, K., Oshima, M. , 2019, ‘‘Computational Simulation of Flow-Induced Arterial Remodeling of the Pancreaticoduodenal Arcade Associated with Celiac Artery Stenosis’’, *Journal of Biomechanics*, Vol.92, pp. 146-154.

[10] Kobayashi, M., Hoshina, K., Nemoto, Y., Takagi, S., Shojima, M., Hayakawa, M., Yamada, S., Oshima, M., 2020, ‘‘A Penalized Spline Fitting Method to Optimize Geometric Parameters of Arterial Centerlines Extracted from Medical Images’’, *Computerized Medical Imaging and Graphics*, Vol.84, pp. 101746..

[11] Kobayashi, M., Hoshina, K., Yamamoto, S., Nemoto, Y., Akai, T., Shigematsu, K., Watanabe, T., Oshima, M., 2015, ‘‘Development of an Image-Based Modeling System to Investigate Evolutional Geometric Changes of a Stent Graft in an Abdominal Aortic Aneurysm’’, *Circulation*

- Journal, Vol.79, pp. 1534-1541.
- [12] Olufsen, M. S., Peskin, C. S., Kim, W. Y., Pedersen, E. M., Nadim, A., Larsen, J., 2003, "Numerical Simulation and Experimental Validation of Blood Flow in Arteries with Structured-Tree Outflow Conditions", *Ann Biomed Eng.* Vol.28, pp.1281-1299.
- [13] Young, D. F., Tsai, F. Y., 1973, "Flow Characteristics in Models of Arterial Stenoses—i. Steady Flow", *J Biomech.* Vol.6., pp.395-402.
- [14] Young, D. F., Tsai, F. Y., 1973, "Flow Characteristics in Models of Arterial Stenoses—ii. Unsteady Flow", *J Biomech.*, Vol.6, pp.547-559.
- [15] Bessems, D., 2007, "On the Propagation of Pressure and Flow waves through the patient-specific arterial system", PhD Thesis, Technische Universiteit Eindhoven, Eindhoven, Netherlands.
- [16] Seeley, B. D., Young, D. F., 1976, "Effect of Geometry on Pressure Losses across Models of Arterial Stenoses". *J Biomech.*, Vol.9, pp.439-446.
- [17] Heinen S. G. H., van den Heuvel D. A. F., de Vries J. P. P. M., van de Vosse, F. N., Delhaas, T., Huberts, W. A., 2019, "Geometry-Based Model for Non-Invasive Estimation of Pressure gradients over iliac artery stenoses. *J Biomech.*, Vol.92, pp.67-75.
- [18] Sankaran, S., Marsden, A.L., 2011, "A stochastic collocation method for uncertainty quantification and propagation in cardiovascular simulations", *J Biomech. Eng.*, Vol. 133, pp.031001.
- [19] Schiavazzi, D.E., Doostan, A., Iaccarino, G., Marsden, A.L., 2017, "A generalized multi-resolution expansion for uncertainty propagation with application to cardiovascular modeling", *Comput. Methods Appl. Mech. Eng.*, Vol.314, pp.196-221.
- [20] Seo, J, Schiavazzi, D.E., Kahn, A.M., Marsden, A.L., 2020, "The effects of clinically-derived parametric data uncertainty in patient-specific coronary simulations with deformable walls", *Int. J Numer. Method Biomed Eng.*, Vol.36, DOI: 10.1002/cnm.3351.
- [21] Xiu D, Sherwin S.J., 2007, "Parametric uncertainty analysis of pulse wave propagation in a model of a human arterial network", *J Comput. Phys.*, Vol.226, pp.1385-1407.
- [22] Chen, P., Quarteroni, A., Rozza, G., 2013, "Simulation-based uncertainty quantification of human arterial network hemodynamics", *Int. J Numer. Method Biomed Eng.*, Vol.29(6), pp.698-721.
- [23] Zhu, Y., Zabaras, N., 2018, "Bayesian deep convolutional encoder–decoder networks for surrogate modeling and uncertainty quantification", *J Comput. Phys.*, Vol.366, pp.415-447.
- [24] Tripathy, R.K., Billionis, I., 2018, "Deep UQ: learning deep neural network surrogate models for high dimensional uncertainty quantification", *J Comput. Phys.*, Vol. 375, pp.565-588.
- [25] Liang, L., Mao, W., Sun, W., 2020, "A feasibility study of deep learning for predicting hemodynamics of human thoracic aorta", *J Biomech.*, Vol.99, pp.109544.
- [26] Sankaran, S., Grady, L., Taylor, C.A., 2015, "Impact of geometric uncertainty on hemodynamic simulations using machine learning", *Comput. Methods Appl. Mech. Eng.*, Vol.297, pp.167-190.
- [27] Itu, L., Rapaka, S., Passerini, T., et al., 2016, "A machine-learning approach for computation of fractional flow reserve from coronary computed tomography", *J Appl Physiol.*, Vol.121, pp.42-52.
- [28] Yuhn, C., Oshima, M., Chen, Y., Hayakawa, M., Yamada, S., 2022, "Uncertainty Quantification in Cerebral Circulation Simulation Focusing on Collateral Flow: Surrogate Model Approach with Machine Learning", *PLOS Comput. Biol.*, DOI: [10.1371/journal.pcbi.1009996](https://doi.org/10.1371/journal.pcbi.1009996).